Article

Development of Oral, Potent, and Selective CK1α Degraders for AML Therapy

Lu Huang, Lu Chen, Lu Chen, Bo Peng, Lixin Zhou, Yanli Sun, Taiting Shi, Jiayi Lu, Weiye Lin, Yuhang Liu, Linhui Cao, Lanlan Li, Qiangqiang Han, Xi Chen, Ping Yang, Shuo Zhang, Zhe Wang, Jing Yang, Zhixiang Guo,* Baishan Jiang,* and Wenchao Lu*

Read Online

ACCESS | Metrics & More | Article Recommendations | SI Supporting Information

ABSTRACT: Molecular glue degraders (MGDs) are proximity-inducing agents that mediate the cooperative interaction between a target protein and an E3 ligase, introducing an additional layer of specificity beyond that afforded by traditional small molecules. Historically, molecular glues that stabilize protein−protein interactions were often discovered serendipitously. In this study, we leveraged the reprogramming potential of cereblon (CRBN)-based ligands and conducted a CRBN-dependent proliferation screen to identify CRBN-based MGDs capable of inducing the degradation of proteins essential for cell viability. Through our screening and subsequent medicinal chemistry optimization, we identified dCK1α-1 as a potent and selective CK1α-targeting molecular glue degrader. Furthermore, we synthesized an orally active derivative, dCK1α-2, with enhanced pharmacokinetic properties, which exhibited pronounced degradation activity and demonstrated efficacy in mouse models following oral gavage. These findings indicate that phenotypic drug discovery campaigns, in combination with chemically distinct CRBN ligand libraries, can accelerate the development of therapeutically relevant MGDs. Furthermore, the development of dCK1α-1 and dCK1α-2 provides new therapeutic options for cancers with functional p53 signaling and offers valuable chemical tools for future investigations into the role of CK1α.

KEYWORDS: molecular glue, CK1α, AML, degrader, induced proximity, P53
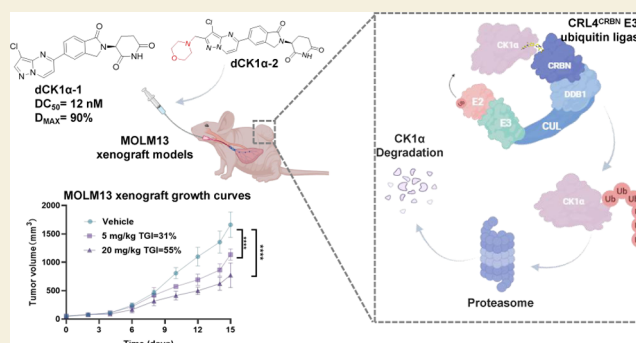
INTRODUCTION

The p53 protein, encoded by the *TP53* gene, is commonly referred to as the "guardian of the genome" because of its pivotal role in responding to DNA damage and other cellular stressors.[1] In mammals, the activity and stability of p53 are tightly regulated by a range of biological processes, including cell proliferation, DNA damage repair, apoptosis, and aging.[2] In human cancers, TP53 is the most frequently mutated tumor suppressor gene, and its alterations are strongly associated with cancer progression. In de novo acute myeloid leukemia (AML), approximately 10% of cases harbor *TP53* mutation.[3] Thus, activating p53 signaling pathways to induce apoptosis represents a promising strategy for improving outcomes in AML patients with wild-type functional p53.

Casein kinase 1A1 (CK1α) is a member of the highly conserved serine/threonine kinase family, phosphorylating a variety of substrate proteins involved in key survival pathways, including the p53, Wnt/β-catenin, and ATM (Ataxia Telangiectasia Mutated Protein) pathways. CK1α has been reported to negatively regulate p53 activity by forming an active complex with the ubiquitin ligases of the murine double minute (MDM) family proteins.[4] In patients with acute myeloid leukemia (AML), mRNA levels of CSNK1A1 (which encodes CK1α) are elevated compared to healthy donors, and aberrant CK1α expression is strongly correlated with reduced overall survival.[5] Genetic knockdown of CSNK1A1 via shRNA or pharmacological inhibition of CK1α using the small-molecule inhibitor D4476 selectively inhibits AML cell proliferation and induces p53-related gene expression, highlighting the therapeutic potential of targeting CK1α in AML therapy.[6] In solid tumors, such as nonsmall-cell lung cancer (NSCLC), CK1α depletion has been shown to inhibit tumor growth by inducing autophagy and enhancing the stability of the tumor suppressor PTEN.[7] CK1α has also been implicated in resistance to enzalutamide in prostate cancer[8] and erlotinib in NSCLC.[9] Recently, an academic-industry collaboration led
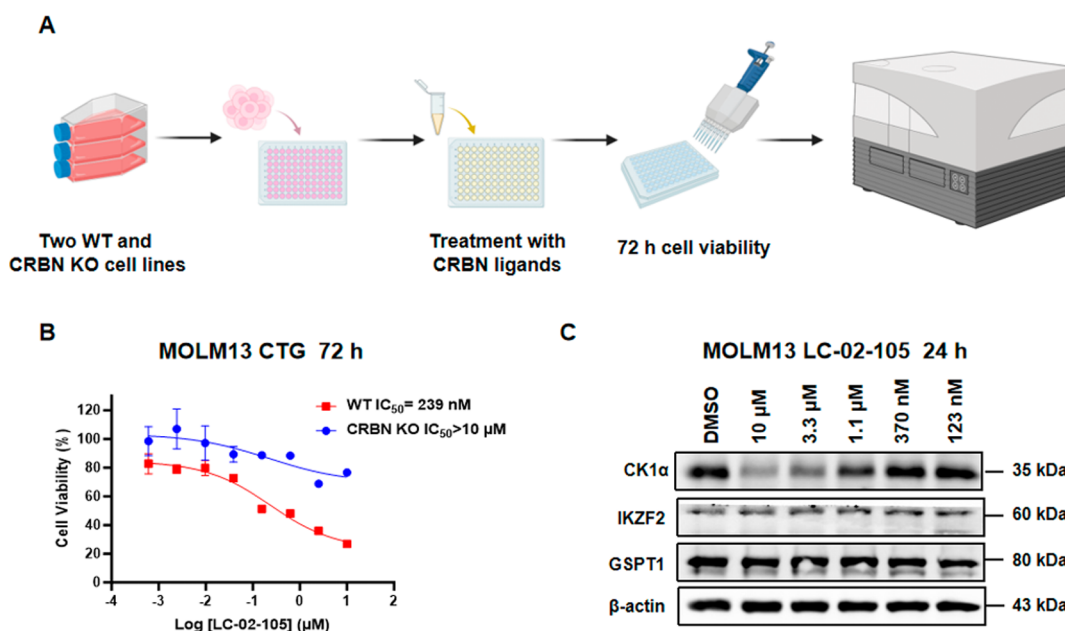
Figure 1. Identification of CK1α MGDs. (A) Schematic representation of the screening flowchart. (B) Viability assay in MOLM13 CRBN^{WT} and CRBN^{KO} cells treated with LC-02−105 for 72 h with biological triplicates. Data are representative of three separate experiments. (C) Immunoblot analysis for CK1α, IKZF2 and GSPT1 in MOLM13 cells treated with LC-02−105 for 24 h at indicated concentrations. Data are representative of three separate experiments.

by Corsello et al.[10] reported the discovery of BAY-888 and BAY-204, potent and selective ATP-competitive CK1α inhibitors with nanomolar potency. In PRISM barcoded cell line screenings, these BAY inhibitors demonstrated promising efficacy beyond AML, phenocopying the effects of short hairpin RNAs (shRNAs)-mediated CK1α knockdown.

Immunomodulatory imide drugs (IMiDs) are small molecules that degrade proteins by co-opting the CUL4-DDB1-CRBN (CRL4^{CRBN}) E3 ubiquitin ligase complex.[11] Thalidomide, lenalidomide, and pomalidomide are the clinically approved IMiDs. Lenalidomide is the only FDA-approved drug known to degrade CK1α, although with limited potency. A seminal study by Ebert et al. demonstrated that lenalidomide induces the ubiquitination and degradation of CK1α in del(5q) myelodysplastic syndromes (MDS), where haploinsufficient CK1α expression enhances sensitivity to lenalidomide therapy.[12] In 2023, Woo et al. developed dual degraders targeting both CK1α and IKZF2, which significantly inhibited cancer progression in AML mouse models and showed therapeutic potential in other cancers, including endometrioid ovarian cancer and diffuse large B-cell lymphoma (DLBCL).[13,14] More recently, Rankovic and colleagues at St. Jude reported the discovery of SJ3149, a potent CK1α degrader exhibiting strong antiproliferative activity across a broad range of human cancer cell lines.[15] These advancements underscore the growing interest in targeting CK1α as a therapeutic strategy for a variety of malignancies.

In our previous work, we demonstrated that the chemical derivatization of triazole-containing IMiD derivatives through click chemistry could rapidly yield selective degraders by reprogramming the substrate specificity of CUL4^{CRBN}.[16] Herein, we identified a series of potent and selective CK1α degraders acting through CRL4^{CRBN} E3 complexes from a paired cell proliferation screen utilizing a focused CRBN-based molecular glue degrader (MGD) library. Among this series, dCK1α-1 emerged as a standout, capable of degrading CK1α

with single-digit nanomolar potency, resulting in robust pharmacological activity against AML cells while exhibiting negligible effects on human PBMCs. Subsequent medicinal chemistry efforts resulted in the development of dCK1α-2, an effective orally bioavailable CK1α degrader. dCK1α-2 is a potent, selective, and *in vivo* compatible chemical tool that demonstrates robust efficacy in degrading CK1α and exhibits excellent compatibility in xenograft mouse models.

■ RESULTS

Discovery of CK1α MGDs from Antiproliferative Phenotypic Screening

To identify potential molecular glue degraders (MGDs) capable of selectively inducing cytotoxicity in cancer cells through a CRBN-dependent mechanism, we screened an in-house proprietary library of CRBN ligands featuring the glutarimide pharmacophore. The screening was performed in a 72-h cell viability assay using both CRBN wild-type (WT) and CRBN-null HEK293T and MOLM13 cell lines (Figure 1A). Lenalidomide and CC-885 served as control compounds. As anticipated, lenalidomide exhibited minimal activity, while the reported degrader CC-885 displayed a nonselective profile, impairing translation termination by targeting G1 to S phase transition protein 1 (GSPT1) (Figure S1A).[17] Among the tested compounds, LC-02−105 emerged as a notable candidate, demonstrating CRBN-dependent cytotoxicity and selectively inducing cell death in MOLM13 cells (acute myeloid leukemia) at an IC$_{50}$ value of 239 nM, while sparing HEK293T cells (Figure 1B).
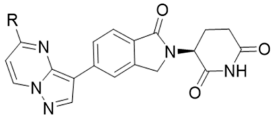
To further elucidate the targets of LC-02−105, we assessed its degradation potency against known essential IMiD targets, including GSPT1, Wee1-like protein kinase (WEE1), and CK1α, which are critical for cancer cell viability, as indicated by the DepMap database (Figures 1C and S1B). Our analysis revealed significant degradation of CK1α, while GSPT1 was spared. WEE1 was not detected, likely due to its relatively low
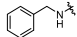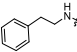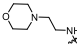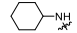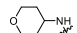
expression levels in MOLM13 cells. Notably, LC-02−105 exhibited minimal effects on IKZF2, which has been reported as an off-target for CK1α degraders.[14]

Optimization of CK1α MGDs

Given the modest activity of LC-02−105, a variety of analogues were synthesized to enhance potency further (Table 1). To support the structure−activity relationship

Table 1. Chemical Modifications on Series 1[ab]

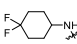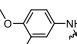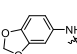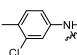| Compound	R	IC$_{50}$ (nM)	DC$_{50}$ (nM)	Dmax (%)
LC-02-047-P2	Cl	>100	>1000	50
LC-02-116		>100	>1000	30
LC-02-117		>100	>1000	0
LC-02-148		>100	>1000	0
LC-02-119		>100	>1000	9
LC-02-120		>100	>1000	14
LC-02-135		>100	>1000	0
LC-02-121		>100	>1000	1
LC-02-104		>100	>1000	0
LC-02-105		>100	>1000	68

[a]Antiproliferation activity was evaluated in MOLM13 cells (72 h) in biological triplicates. CK1α MGDs were dosed starting at a concentration of 100 nM, followed by a 7-point, 3-fold serial dilution. [b]Degradation activity was evaluated in a CK1α HiBiT MOLT4 cell line (24 h) in biological triplicates. DC$_{50}$ was determined with doses starting from 10 μM, followed by an 8-point, 3-fold serial dilution. D_{max} was determined using nonlinear regression curves in GraphPad PRISM 9.5.

(SAR) efforts for this series of compounds, we established CRISPR/Cas9-modified MOLT4 cells with endogenously HiBiT-tagged CK1α to efficiently screen degradation potency using an end point luciferase assay, while simultaneously validating degradation through Western blots at 100 nM and 20 nM in MOLM13 cells, respectively (Figures 2 and S2). Additionally, an antiproliferation assay with MOLM13 cells was conducted to ensure that the degradation activity translates to the desired efficacy (Figure S3).

Given that the phthalimide core was deemed unsuitable for CK1α degradation, we retained the isoindolinone core and focused our efforts on modifying the pyrazolopyrimidine substitutions. Initially, replacing the methyl group of LC-02−105 with a methoxy group or introducing a ring-closed aniline resulted in the synthesis of LC-02−121 and LC-02−104,

respectively. Additionally, substituting the R group with cyclohexylamine, 4-aminotetrahydropyran, or 1,1-difluorocyclohexylamine yielded compounds LC-02−119, LC-02−120, and LC-02−135. Switching to analogues of phenylmethanamine, phenylethane-1-amine, or morpholinoethan-1-amine afforded LC-02−116, LC-02−117, and LC-02−148, respectively. A chlorine-substituent analogue, LC-02−047-P2, was also synthesized. The first series of derivatives was then subjected to immunoblot analysis at fixed doses of 20 nM and 100 nM, and was also evaluated using the HiBiT assay in leukemia cells. Unexpectedly, none of the structural variations exhibited improved inhibitory activity, suggesting a steep structure−activity relationship (SAR), a phenomenon commonly observed with molecular glue degraders.

Given the minimal improvement in activity from the initial efforts, we concentrated on second-round optimization. This optimization involved changing the attachment point of the isoindolinone moiety from the 3-position to the 6-position of the pyrazolo[1,5-a] pyrimidine group, resulting in the LC-04−075 series (Table 2). Notably, LC-04−075 demonstrated the ability to degrade CK1α with a half-maximal degradation (DC$_{50}$) value of 141 nM. The introduction of halogen atoms, such as bromide (LC-02−47-P1) or chloride (LC-04−087), at the R1 position significantly increased potency and antiproliferative activity, whereas switching to amino (LC-04−081) or nitrile substitutions (LC-04−077) compromised potency. The introduction of a methyl group at the R2 position was well tolerated, as illustrated by the similar activities of compounds LC-04−075 and LC-04−155, as well as LC-04−087 and LC-04−162. Among this series, LC-04−087 proved to be the most potent CK1α MGD, exhibiting high ligand efficiency (LE) and reducing CK1α abundance with a DC$_{50}$ value of 12 nM and a Dmax of 90% (Figure S3). We subsequently renamed this potent chemical probe dCK1α-1.

To further elucidate the observed structure−activity relationship and gain structural insights into ternary complex formation, we conducted in silico docking analyses using Maestro 13.5 (Schrödinger, New York). The resulting complex resembles previously determined CK1α-CRBN ternary complexes, in which the aromatic cage/tritryptophan pocket (W380, W386, and W400) accommodates the glutarimide ring.[15,18] The isoindolinone core of dCK1α-1 forms a series of hydrogen bond interactions with CRBN through H378 and N351. The model also suggests a potential hydrogen bonding interaction between the pyrazolo[1,5-a] pyrimidine group and H353, which further enhances cooperativity (Figure 3A). Based on the binding conformation of dCK1α-1 in the docking model, there are no obvious interactions with the key residue IKZF2-H141, which may explain the selectivity for CK1α over IKZF2. We also conducted a NanoBiT assay to confirm the ability of dCK1α-1 to induce ternary complex formation between CRBN and CK1α. The results indicate that dCK1α-1 can achieve up to 1500% recruitment at a concentration of 4 μM (Figure 3B).

dCk1α-1 Is a Potent and Selective MGD against CK1α

To further confirm that the observed phenotype is CRBN-dependent, we evaluated degradation in both wild-type and CRBN-null MOLM13 cells. As anticipated, dCK1α-1 induced significant degradation in wild-type MOLM13 cells while sparing CRBN-null MOLM13 cells (Figure 3C). The degradation event could be rescued by pretreatment with MLN4924 (a Cullin neddylation inhibitor), bortezomib (a
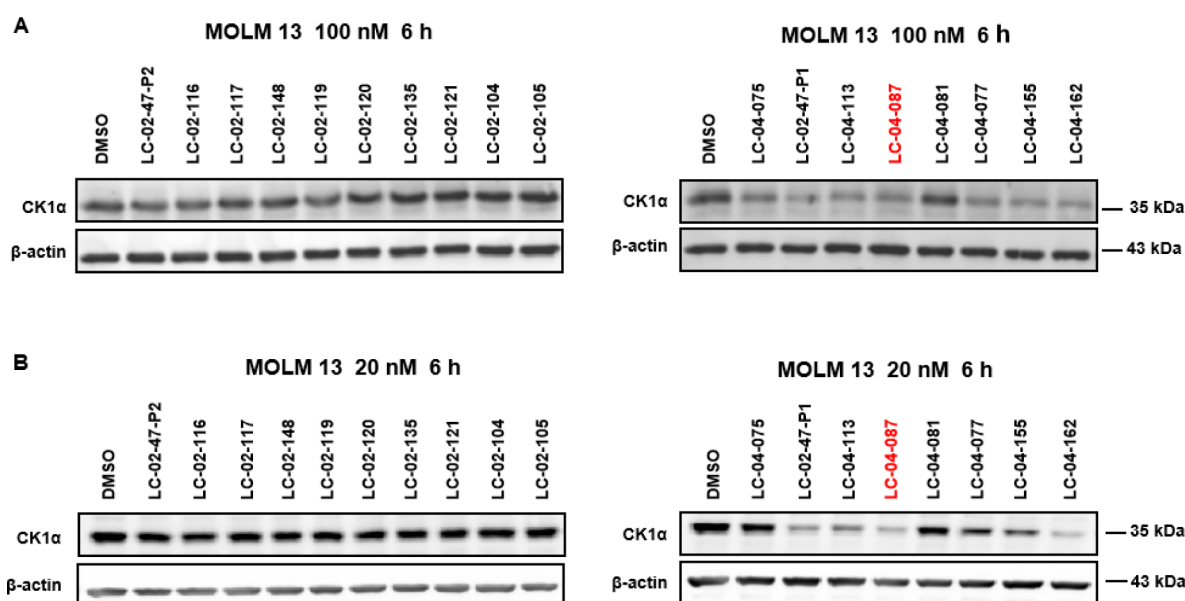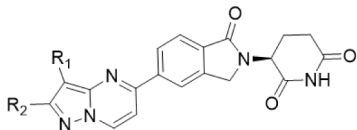
Figure 2. Immunoblot analysis of CK1α degradation in MOLM13 cells. Cells were treated with CK1α MGDs for 6 h at (A) 100 nM and (B) 20 nM, respectively. Data are representative of three independent experiments.

Table 2. Chemical Modifications on Series 2[a,b]

Compound	R1	R2	IC$_{50}$ (nM)	DC$_{50}$ (nM)	Dmax (%)
LC-04−075	H	H	>100	141	79
LC-02-047-P1	Br	H	13	14	86
LC-04-113	Me	H	32	10	91
LC-04-087	Cl	H	8	12	90
LC-04-081	NH2	H	>100	>1000	31
LC-04-077	CN	H	>100	406	93
LC-04-155	H	Me	>100	90	83
LC-04-162	Cl	Me	8	12	89

[a]Antiproliferation activity was evaluated in MOLM13 cells (72 h) in biological triplicates. CK1α MGDs were dosed starting at a concentration of 100 nM, followed by a 7-point, 3-fold serial dilution. [b]Degradation activity was evaluated in a CK1α-HiBiT MOLT4 cell line (24 h) in biological triplicates. DC$_{50}$ was determined with doses starting from 10 μM, followed by an 8-point, 3-fold serial dilution. D_{max} was determined using nonlinear regression curves in GraphPad PRISM 9.5.

proteasome inhibitor), or pomalidomide (a CRBN competitor), confirming that the observed degradation was mediated by the CUL4^{CRBN} ubiquitin pathway (Figure 3D). To further assess the kinetics of CK1α degradation, we conducted a time-course study using 100 nM dCK1α-1 in MOLM13 cells. The results indicated that degradation occurred as early as 2 h and persisted for at least 24 h (Figure 3E). Consistent with the HiBiT data from MOLT4 cells, dCK1α-1 completely degraded CK1α in MOLM13 cells, with minimal effects on IKZF2 and GSPT1, which are known off-targets in the development of CK1α MGDs (Figure 3F). Additionally, a concomitant increase in p53 and p21 protein levels was observed, demonstrating the on-target effect on the p53 signaling pathway. To further explore the selectivity profile of dCK1α-1 in MOLM13 cells, we conducted a tandem mass tag (TMT)-based quantitative mass spectrometry (MS) proteomic study. As shown in Figure 3G, treatment with 1 μM dCK1α-1 for 6 h revealed that CK1α was the most prominent hit among over 9,000 proteins. Notably, significant upregulation of β-catenin was also observed, supporting CK1α's role in regulating the p53 and β-catenin signaling pathways. Furthermore, PRISM data from our previously reported CK1α-degrading agent, TMX-4116, clearly indicated that hematological disease cell lines are particularly sensitive to CK1α degradation[16] (Figure S4). We also evaluated the antiproliferative effects of dCK1α-1 in 13 selected representative cell lines, including HCT116 (colon cancer), A549 (lung cancer), and HEK293T (embryonic kidney). dCK1α-1 exhibited selective inhibition in AML lines such as MOLM13 and MV4−11, while sparing human peripheral blood mononuclear cells (PBMCs), demonstrating a high safety profile (Figure S5).

dCk1α-1 Sensitizes AMG-232 in AML Cells

Next, we evaluated the effects of the degrader on cell cycle progression and apoptosis in AML cells using flow cytometry. As shown in Figure 4A, dCK1α-1 induced apoptosis and caused cell cycle arrest at the G1 phase in a dose-dependent manner. Additionally, we observed a significant upregulation of cleaved caspase-3, indicating the activation of apoptosis (Figure S6). Given the observed activation of p53 signaling in MOLM13 cells, we hypothesized that dCK1α-1 may have potential when combined with MDM2 inhibitors. To test this hypothesis, we assessed the antiproliferative activity in MOLM13 cells treated with dCK1α-1 and navtemadlin (AMG-232), a reported MDM2 inhibitor, over 3 days. A highest single agent (HSA) model was employed to determine whether the observed combinatorial effect was synergistic.[19] As expected, a strong synergistic effect was observed, accompanied by increased apoptosis in the combination group (Figure 4B-D). We also evaluated the combinatorial effects of dCK1α-1 and navtemadlin in the DLD-1 (colorectal adenocarcinoma), T98G (glioblastoma), and HEK293T (immortalized human embryonic kidney) cell lines. However, we did not observe a significant combinatorial effect in these
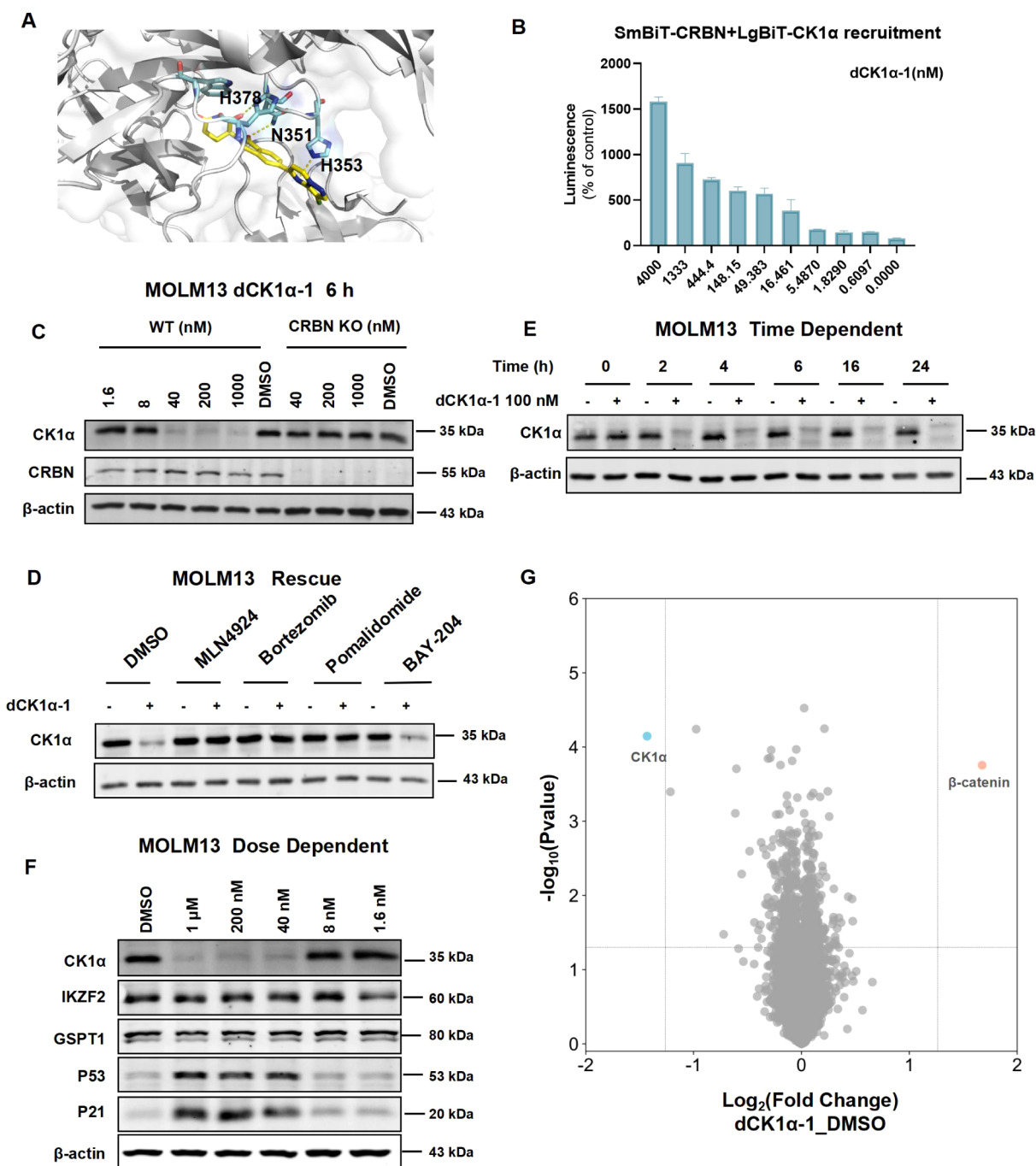
Figure 3. dCK1α-1 Induces Potent, Rapid, Selective, and CRBN-Dependent CK1α degradation in MOLM13 cells. (A) Docking model of the CK1a-CRBN-DDB1-dCK1α-1 complex. dCK1α-1 is depicted as yellow sticks with hydrogen bonds highlighted in yellow dashes. (B) Ternary complex formation was assessed in HEK293T cells with increasing doses of dCK1α-1 after 4 h treatment. (C) Immunoblot analysis of MOLT4 parental or CRBN-null cells treated with dCK1α-1 for 6 h. (D) Immunoblot analysis of MOLM13 cells pretreated with DMSO, MLN4924, Bortezomib, pomalidomide, or BAY204 for 1 h, and then cotreated with 100 nM dCK1α-1 for 6 h. (E) Time-dependent analysis of degradation activity of dCK1α-1 in MOLM13 cells. (F) Immunoblot analysis of MOLM13 cells treated with dCK1α-1 at the indicated concentrations for 24 h. (G) Whole-cell proteomic study of dCK1α-1 in MOLM13 cells. Cells were treated with 1 μM dCK1α-1 for 6 h. Experiments were conducted in three biological replicates.

cell lines, suggesting that the combination of the MDM2 inhibitor and CK1α degrader may be particularly beneficial in AML cells, such as MOLM13 (Figure S7).

dCk1α-1 Activated p53 Apoptosis Pathway by Induced CK1α Degradation

To further elucidate the antiproliferative effects of dCK1α-1, we aimed to investigate the transcriptome-wide perturbations induced by this compound. RNA sequencing was performed on MOLM13 cells treated with 200 nM dCK1α-1 or BAY-204, a potent ATP-competitive CK1α inhibitor (Figures 5A and S8). Volcano plots revealed that 2,213 genes were differentially expressed with statistical significance (fold change ≥ 2 and adjusted p-value ≤ 0.05) following dCK1α-1 treatment, with most of these genes overlapping with those in the BAY-204-
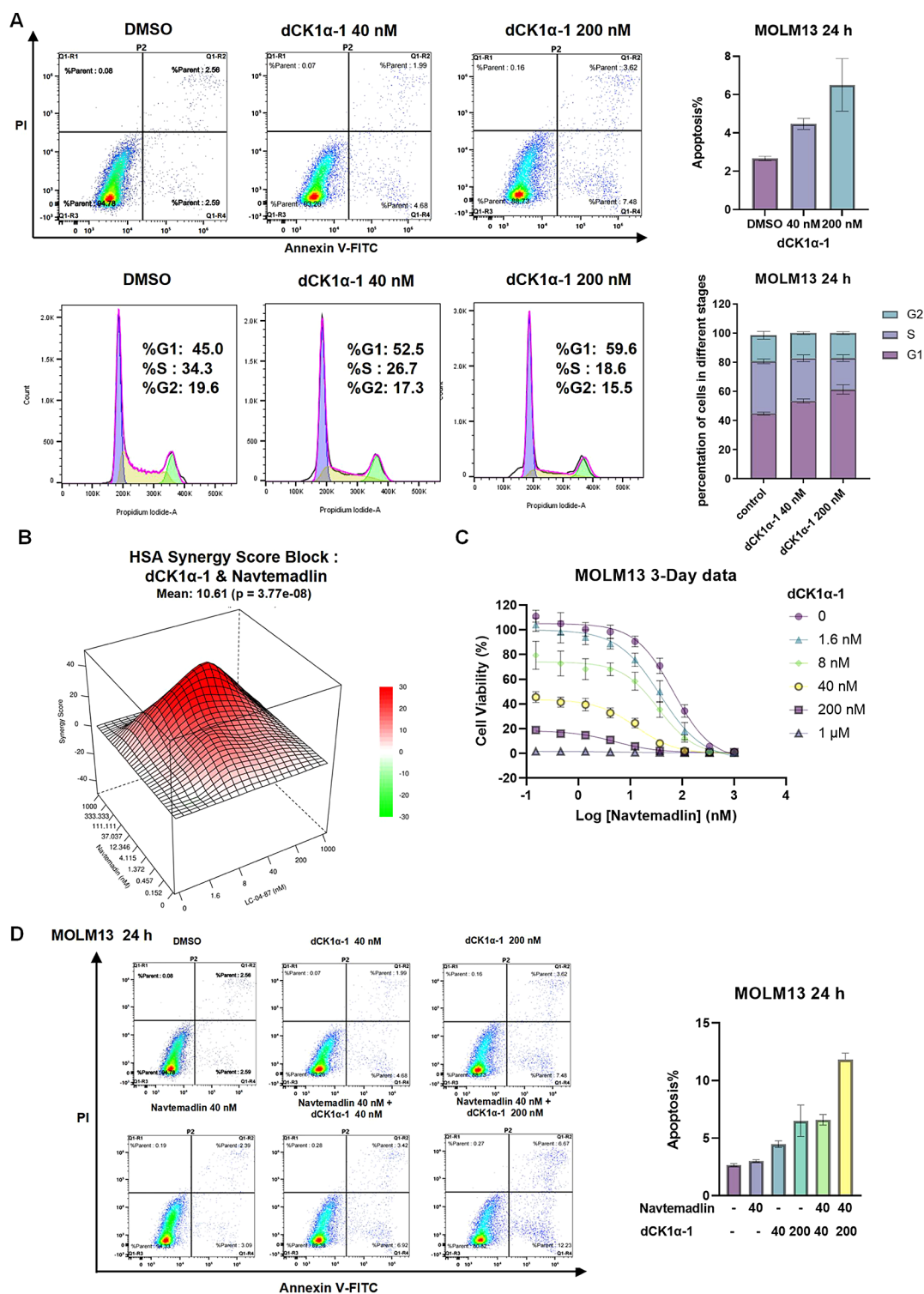
Figure 4. dCK1α-1 Caused Cell Cycle Arrest and Induced Apoptosis in MOLM13 Cells. (A) Evaluation of dCK1α-1 effect on cell cycle and apoptosis by flow cytometry. MOLM13 cells were treated with dCK1α-1 at the indicated concentrations for 24 h. Experiments were conducted with three biological replicates. (B) Excess over HSA synergy plots for dCK1α-1 in combination with Navtemadlin in MOLM13 cells. Experiments were conducted with three biological replicates. (C) Cell viability of MOLM13 cells cotreated with dCK1α-1 and Navtemadlin for 72 h using CellTiter-Glo. Plotted as mean ± SD for n = 3 replicates. (D) The apoptosis effect of MOLM13 cells cotreated with dCK1α-1 and Navtemadlin for 72 h using flow cytometry. Data are representative of three separate experiments.

treated group (Figure 5A,D). In contrast, BAY-204 elicited a more pronounced response, with 5,020 differentially expressed genes (DEGs) identified. To explore whether these DEGs were involved in specific biological pathways, KEGG pathway analysis indicated that these genes were associated with cell cycle regulation, p53 signaling, DNA repair, and other processes (Figure 5B). Additionally, Gene Set Enrichment Analysis (GSEA) revealed significant enrichment of DEGs in the cell cycle, p53 signaling, apoptosis pathway, and MAPK signaling in dCK1α-1-treated cells (Figure 5C). Furthermore,
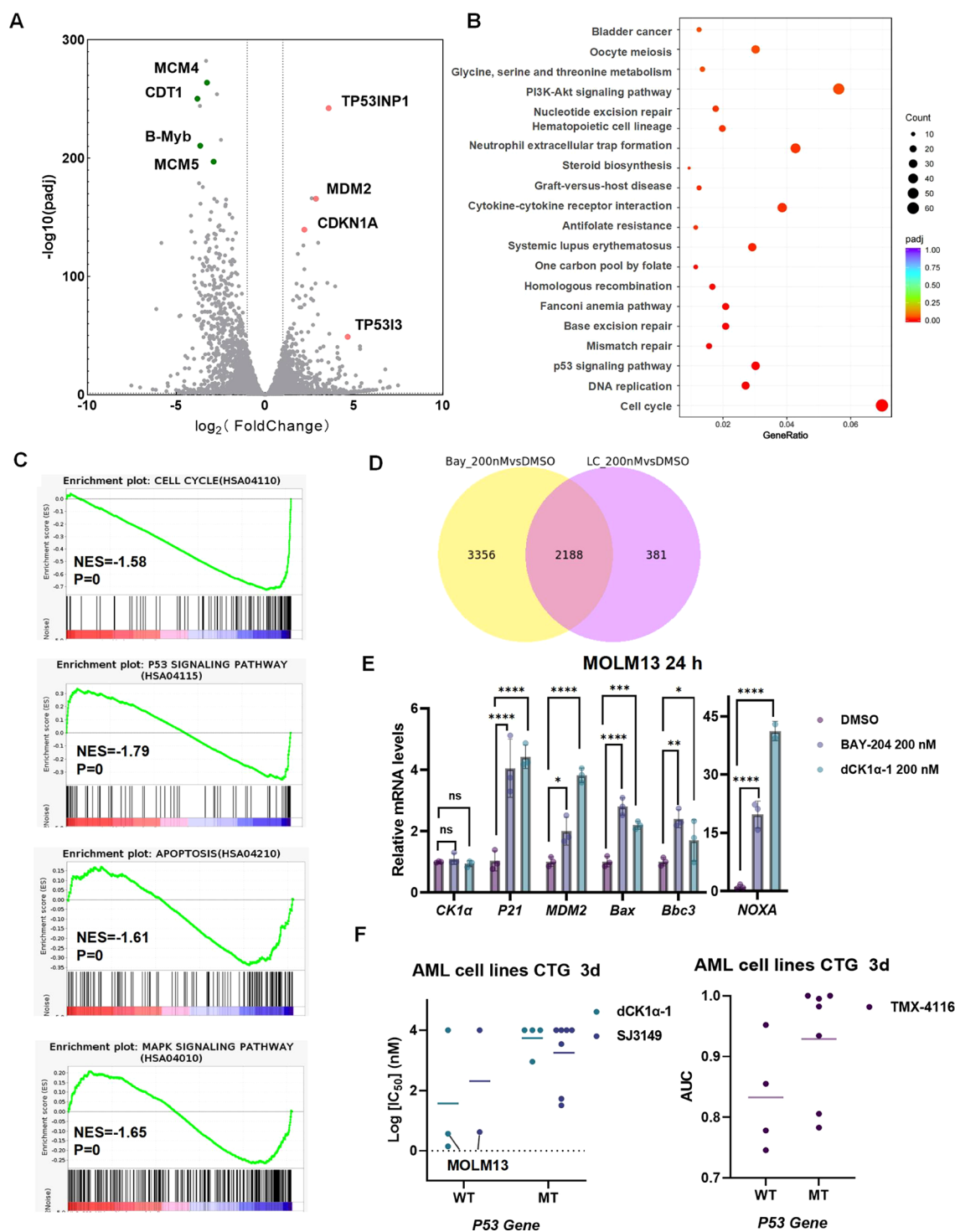
Figure 5. CK1α Inhibition/degradation Activated p53-associated Transcriptional Program in MOLM13 Cells. (A) The volcano plot of gene expression changes for cells treated with dCK1α-1 (CK1α degrader). The differentially expressed genes (DEGs) with FC value greater than 2.0 and p-value smaller than 0.05 were colored in red and selectively labeled. Experiments were conducted with three biological replicates. (B) Pathway enrichment analysis of DEGs from 200 nM dCK1α-1 treatment samples. (C) GSEA plots. NES, normalized enrichment score. (D) Venn diagram of DEGs in dCK1α-1/BAY-204-treated cells. (E) RT-PCR validation on selected genes in MOLM13 cells treated with 200 nM dCK1α-1 or BAY-204 (24 h). Data are representative of three separate experiments. (F) The scatterplots of the IC_{50} distributions of dCK1α-1, SJ3149, and TMX-4116 in AML cell lines. Cell lines were grouped based on their TP53 genotype (wild-type versus mutants). IC_{50} values (in nM) for each cell line are derived from a 3-day proliferation assays with 9 doses in biological duplicates. The data for dCK1α-1 were obtained from proliferation assays, while the data for SJ3149 and TMX-4116 were sourced from respective PRISM data sets.

PRISM analysis of mutation-based sensitivity patterns indicated that deleterious hotspot mutations in *TP53* confer resistance to the antiproliferative activity of the CK1α-degrading agent TMX-4116 (Figure S9). Reverse transcription polymerase chain reaction (RT-qPCR) further confirmed the increased transcription of p53 signature genes, including *p21*,
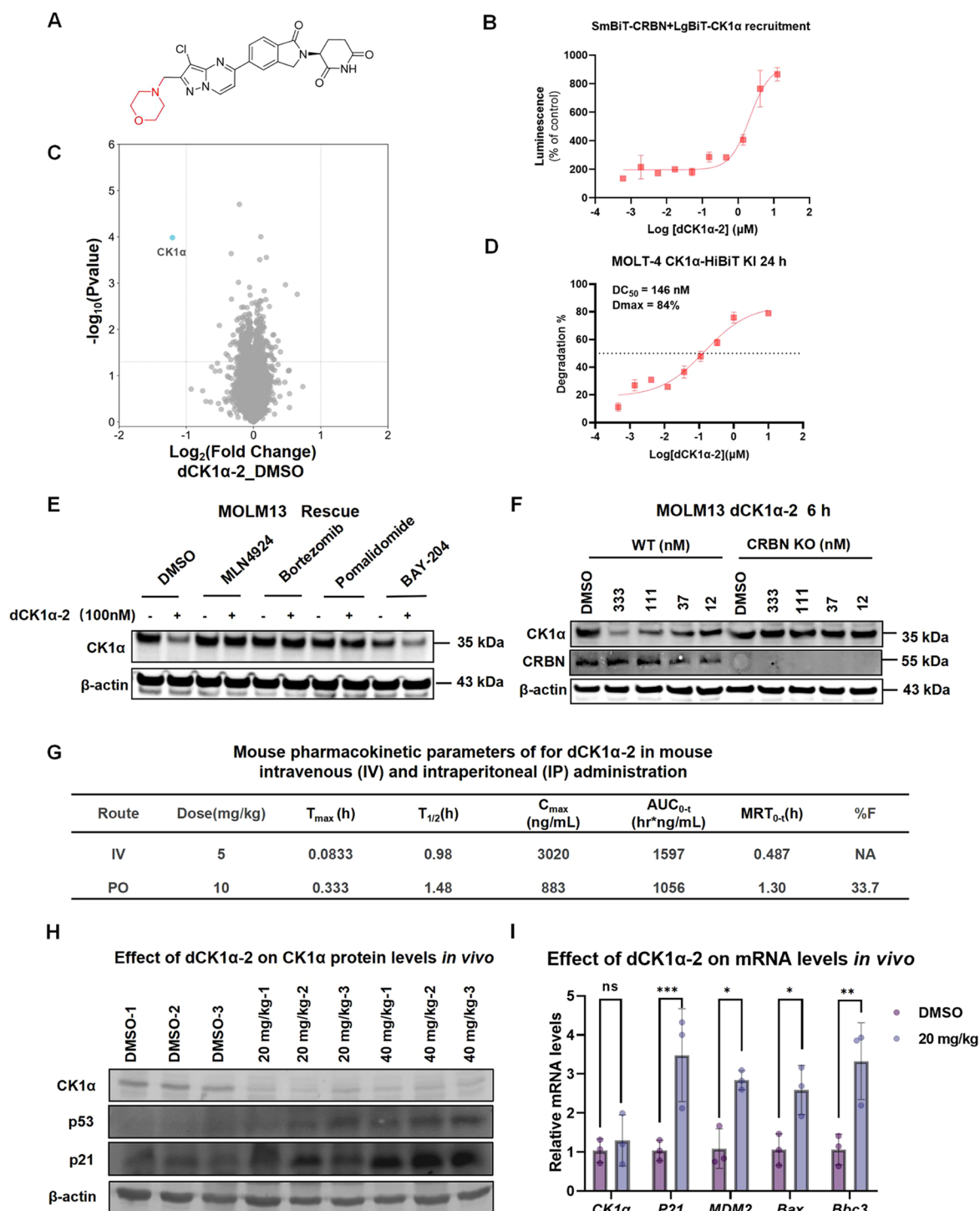
Figure 6. Development of a Potent, Selective and *In-vivo* Compatible CK1α MGD. (A) The chemical structure of dCK1α-2. (B) Ternary complex formation was assessed in HEK293T cells with increasing doses of dCK1α-2 after 4 h treatment. (C) Whole-cell proteomic study of dCK1α-2 in MOLM13 cells. Cells were treated with 1 μM dCK1α-2 for 6 h. Experiments were conducted in three biological replicates. (D) Degradation activity of dCK1α-2. MOLT4 HiBiT-CK1α cells were treated with dCK1α-2 at the indicated concentrations for 24 h. Data are representative of three separate experiments. (E) Immunoblot analysis of MOLM13 cells pretreated with DMSO, MLN4924, bortezomib, pomalidomide, or BAY204 for 1 h, and then cotreated with 100 nM dCK1α-2 for additional 6 h. (F) Immunoblot analysis of MOLT4 parental or CRBN-null cells treated with dCK1α-2 for 6 h. (G) Pharmacokinetic parameters of dCK1α-2 following intravenous (IV) and oral (PO) administration in mouse models. (H) Immunoblot analysis of the effect of dCK1α-2 on CK1α in mice. Data are representative of three separate experiments. (I) qPCR analysis of the effect of dCK1α-2 on p53 target genes in mouse models. Data are representative of three separate experiments.

MDM2, BAX, BBC3, and *NOXA* (Figure 5E). We evaluated the antiproliferative effects of dCK1α-1 across a panel of seven AML cell lines (THP-1, HL-60, MV4−11, U937, Kasumi-1, HEL, MOLM13), incorporating data sets from SJ3149 and

PRISM data from TMX-4116. The results indicated a trend suggesting that dCK1α-1 inhibited the proliferation of TP53 wild-type AML cells more effectively (Figures 5F and S10). However, it is important to note that we cannot conclude that
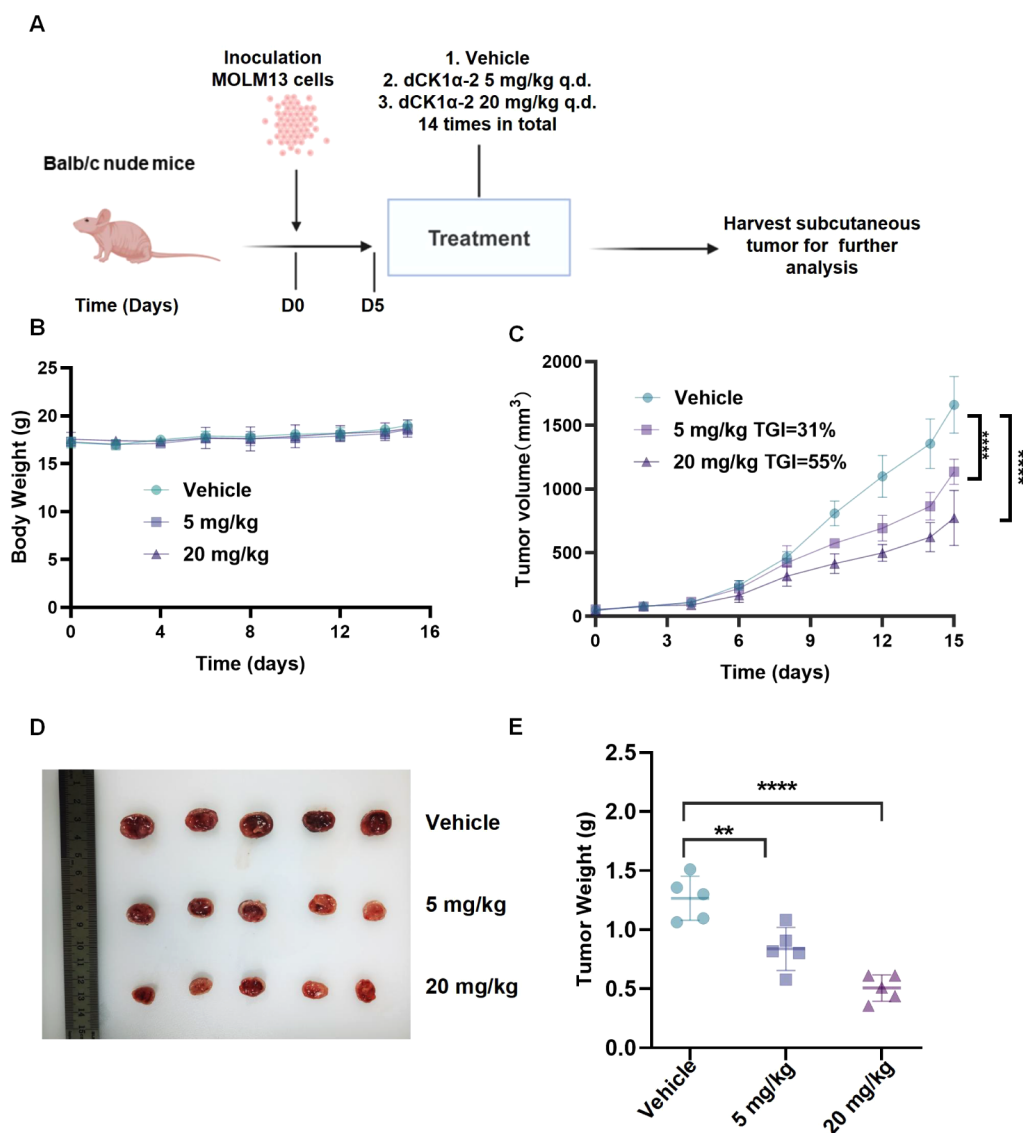
Figure 7. Effects of dCK1α-2 on MOLM13 growth in mouse xenograft models. (A) Schematic diagram of the efficacy study design. (B) Body weights of mice throughout the study (*n* = 5). (C) Tumor growth curves for mice bearing MOLM13 xenografts, treated with either vehicle (DMSO) or dCK1α-2 (5 or 20 mg/kg). Tumor volumes were measured every other day (*n* = 5). (D) Images of the resected xenografts. (E) Weights of the resected xenograft tumors.

TP53 is the sole biomarker for determining sensitivity to CK1α MGDs, considering the complexity of cancer.

A Drug-Like Derivative dCk1α-2 Induced −CK1α Degradation In Vivo

To demonstrate the therapeutic potential of CK1α MGDs, we evaluated the metabolic stability of the dCK1α-1 series in human liver microsomes. dCK1α-1 exhibited favorable metabolic stability, with a half-life of 630 min and a clearance rate of 1.98 mL/min/kg. However, dCK1α-1 exhibited a solubility limitation, with a concentration limit of 20 mM in DMSO. To enhance solubility and facilitate the *in vivo* study of CK1α degradation, a morpholine group was introduced into the solvent exposure region based on the docking model of dCK1α-1, resulting in compound dCK1α-2 (Figures 6A and S11). As expected, dCK1α-2 was capable of inducing ternary complex formation between CRBN and CK1α in HEK293T cells (Figure 6B). Additionally, dCK1α-2 degraded CK1α *in vitro* and demonstrated significant selectivity in TMT proteomic studies in MOLM13 AML cells (Figure 6C,D).

Pretreatment with MLN4924, bortezomib, or pomalidomide rescued the degradation event, and the degradation effect was minimal in CRBN-null MOLM13 cells, further confirming that degradation was mediated by the CUL4CRBN ubiquitin pathway (Figure 6E,F). Following a single oral administration in ICR male mice at 10 mg/kg, dCK1α-2 displayed rapid absorption, with a half-life of 1.48 h and a peak plasma concentration (Cmax) of 883 ng/mL (1.78 μM) (Figure 6G). The oral bioavailability was 34%, which is superior to that of the previously reported CK1α MGD SJ3149 (Figure S12).[15] With promising oral bioavailability data, we advanced dCK1α-2 into pharmacodynamic pilot studies. Tumor-bearing BALB/c nude mice were randomized and orally administered dCK1α-2 once daily at doses of 20 mg/kg and 40 mg/kg for three consecutive days (Figure S13). Significant degradation was observed in dCK1α-2-treated mice, leading to the upregulation of p53-related target gene expression. Notably, no significant change in the expression of CK1α mRNA was observed via reverse transcription quantitative polymerase chain reaction

(RT-qPCR), supporting a post-transcriptional effect on CK1α abundance (Figure 6I).

Encouraged by the pharmacodynamic study results, we selected two dosing regimens (20 mg/kg and 5 mg/kg) for continuous treatment over 14 days in mouse xenograft models bearing MOLM13 cells to further evaluate the *in vivo* antitumor efficacy of dCK1α-2 through oral gavage (Figure 7A). The administration of dCK1α-2 was well tolerated, with minimal impact on body weight (Figure 7B).

Notably, significant tumor regression was observed in the dCK1α-2-treated groups compared to the vehicle-treated controls. The 5 mg/kg group exhibited a tumor growth inhibition rate (TGI) of 31%, whereas the 20 mg/kg group achieved a TGI of 55% (Figure 7C-E). These findings suggest that dCK1α-2 effectively inhibits MOLM13 xenograft tumor growth *in vivo,* with good tolerance observed across all treatment groups. In summary, dCK1α-2 represents an orally bioavailable CK1α molecular glue degrader for p53-related targeted therapy.

■ CONCLUSIONS

The discovery of pharmacological modalities that can activate the p53 pathway has been a long-standing effort in cancer therapy, exemplified by the development of MDM2/p53 inhibitors,[20] allele-specific p53-targeted drugs such as arsenic trioxide (ATO),[21] and p53 Y220C covalent binders.[22] CK1α, a Ser/Thr casein kinase, has been reported to promote MDM2/p53 interactions and sustain tumor growth in leukemia and solid tumors, making it a potential therapeutic target for p53-related cancer treatment. Recent studies have demonstrated that immunomodulatory imide drugs (IMiDs), particularly lenalidomide, are among the therapeutic modalities that can induce CK1α degradation via the CRL4^{CRBN} E3 ligase. Several of these agents are currently undergoing clinical trials, including BMS-986397 (Bristol Myers Squibb, Phase 1, NCT04951778, R/R AML and MDS) and GLB-001 (GluBio Therapeutics, Phase 1, NCT06146257, R/R AML and MDS), demonstrating preliminary therapeutic efficacy in targeting CK1α. Through proliferation screening in CRBN wild-type (WT) and CRBN-null AML cells, followed by medicinal chemistry optimization, we identified dCK1α-1 as a potent and selective CK1α molecular glue degrader with single-digit nanomolar activity. dCK1α-1 displays a strong synergistic effect with the MDM2/p53 inhibitor navtemadlin, which holds great promise for positively impacting outcomes and reducing on-target hematological toxicities associated with other p53 activators through complementary mechanisms. Further optimizations led to the identification of an orally bioavailable and selective derivative, dCK1α-2, which exhibits potent degradation in mouse xenograft models. Although still in its infancy, the development of CK1α molecular glue degraders will deepen our understanding of the pharmacological actions and potential clinical benefits of targeting CK1α, offering therapeutic opportunities for broad anticancer applications beyond leukemia.

■ ASSOCIATED CONTENT

Data Availability Statement

ESI Figures, tables, and experimental details as well as ^{1}H NMR and ^{13}C NMR of compounds are provided in the ESI.

■ Supporting Information

The Supporting Information is available free of charge at https://pubs.acs.org/doi/10.1021/jacsau.4c00762.

(PDF)

(XLSX)

(XLSX)

(XLSX)

■ AUTHOR INFORMATION

Corresponding Authors

Zhixiang Guo — *Department of Cardiovascular Surgery, The First Affiliated Hospital of Anhui Medical University, Hefei 230022, China;* Email: aydgzx100@163.com

Baishan Jiang — *Department of Radiation and Medical Oncology, Medical Research Institute, Frontier Science Center of Immunology and Metabolism, Zhongnan Hospital of Wuhan University, School of Pharmaceutical Sciences, Wuhan University, Wuhan 430071, China;* Email: baishan_jiang@whu.edu.cn

Wenchao Lu — *Lingang Laboratory, Shanghai 200031, China;* orcid.org/0000-0003-1175-365X; Email: luwenchao@lglab.ac.cn

Authors

Lu Huang — *Department of Cardiovascular Surgery, The First Affiliated Hospital of Anhui Medical University, Hefei 230022, China; Lingang Laboratory, Shanghai 200031, China*

Lu Chen — *Department of Radiation and Medical Oncology, Medical Research Institute, Frontier Science Center of Immunology and Metabolism, Zhongnan Hospital of Wuhan University, School of Pharmaceutical Sciences, Wuhan University, Wuhan 430071, China*

Lu Chen — *Lingang Laboratory, Shanghai 200031, China*

Bo Peng — *Lingang Laboratory, Shanghai 200031, China*

Lixin Zhou — *Department of Hematology, Tongji Hospital, Frontier Science Center for Stem Cell Research, Shanghai Key Laboratory of Signaling and Disease Research, School of Life Sciences and Technology, Tongji University, Shanghai 200092, China*

Yanli Sun — *Lingang Laboratory, Shanghai 200031, China*

Taiting Shi — *Lingang Laboratory, Shanghai 200031, China; Department of Neurosurgery, The First Affiliated Hospital of Wenzhou Medical University, Wenzhou 325000, China*

Jiayi Lu — *College of Science, Northeastern University, Boston, Massachusetts 02115, United States*

Weiye Lin — *Lingang Laboratory, Shanghai 200031, China; School of Life Science and Technology, ShanghaiTech University, Shanghai 201210, China*

Yuhang Liu — *Lingang Laboratory, Shanghai 200031, China; School of Pharmacy, Key Laboratory of Molecular Pharmacology and Drug Evaluation (Yantai University), Ministry of Education; Collaborative Innovation Center of Advanced Drug Delivery System and Biotech Drugs in Universities of Shandong, Yantai University, Yantai 264005, China*

Linhui Cao — *Lingang Laboratory, Shanghai 200031, China; School of Pharmacy, Key Laboratory of Molecular Pharmacology and Drug Evaluation (Yantai University), Ministry of Education; Collaborative Innovation Center of Advanced Drug Delivery System and Biotech Drugs in*

Universities of Shandong, Yantai University, Yantai 264005, China

Lanlan Li − *Lingang Laboratory, Shanghai 200031, China; Institute of Entomology, The Provincial Special Key Laboratory for Development and Utilization of Insect Resources, Guizhou University, Guiyang 550025, China*

Qiangqiang Han − *SpecAlly Life Technology Co., Ltd., Wuhan 430075, China*

Xi Chen − *SpecAlly Life Technology Co., Ltd., Wuhan 430075, China*

Ping Yang − *Department of Cardiovascular Surgery, The First Affiliated Hospital of Anhui Medical University, Hefei 230022, China*

Shuo Zhang − *Department of Cardiovascular Surgery, The First Affiliated Hospital of Anhui Medical University, Hefei 230022, China*

Zhe Wang − *Department of Cardiovascular Surgery, The First Affiliated Hospital of Anhui Medical University, Hefei 230022, China*

Jing Yang − *Department of Hematology, Tongji Hospital, Frontier Science Center for Stem Cell Research, Shanghai Key Laboratory of Signaling and Disease Research, School of Life Sciences and Technology, Tongji University, Shanghai 200092, China*

Complete contact information is available at:
https://pubs.acs.org/10.1021/jacsau.4c00762

Author Contributions

▶L.H., L.Chen, and L.Chen contributed equally to this work. W.L., B.J., and Z.G. designed the study. L.H., L.Chen, B.P., T.S., J.L., W.L., Y.L., L.C., L.L., P.Y., S. Z., Z.W., Y.S., and J.Y. carried out *in vitro* experiments, collected and analyzed the data. L.Z. did molecular docking studies. Q.H., X.C. performed proteomics studies. L.H., L. Chen, B.J., and W.L. wrote the manuscript. All authors have read and approved the article.

Notes

The authors declare no competing financial interest.

■ REFERENCES

(1) Levine, A. J. p53, the cellular gatekeeper for growth and division. *Cell* **1997**, *88* (3), 323−331.
(2) Kastenhuber, E. R.; Lowe, S. W. Putting p53 in Context. *Cell* **2017**, *170* (6), 1062−1078.
(3) Rucker, F. G.; Schlenk, R. F.; Bullinger, L.; Kayser, S.; Teleanu, V.; Kett, H.; Habdank, M.; Kugler, C. M.; Holzmann, K.; Gaidzik, V. I. TP53 alterations in acute myeloid leukemia with complex karyotype correlate with specific copy number alterations, monosomal karyotype, and dismal outcome. *Blood* **2012**, *119* (9), 2114−2121.

(4) (a) Ball, B.; Abdel-Wahab, O. Activating p53 and Inhibiting Superenhancers to Cure Leukemia. *Trends Pharmacol. Sci.* **2018**, *39* (12), 1002−1004. (b) Huart, A. S.; MacLaine, N. J.; Meek, D. W.; Hupp, T. R. CK1alpha plays a central role in mediating MDM2 control of p53 and E2F-1 protein stability. *J. Biol. Chem.* **2009**, *284* (47), 32384−32394.
(5) Xu, W.; Huang, Z.; Gan, Y.; Chen, R.; Huang, Y.; Xue, B.; Jiang, S.; Yu, Z.; Yu, K.; Zhang, S. Casein kinase 1alpha inhibits p53 downstream of MDM2-mediated autophagy and apoptosis in acute myeloid leukemia. *Oncol. Rep.* **2020**, *44* (5), 1895−1904.
(6) Jaras, M.; Miller, P. G.; Chu, L. P.; Puram, R. V.; Fink, E. C.; Schneider, R. K.; Al-Shahrour, F.; Pena, P.; Breyfogle, L. J.; Hartwell, K. A. Csnk1a1 inhibition has p53-dependent therapeutic efficacy in acute myeloid leukemia. *J. Exp. Med.* **2014**, *211* (4), 605−612.
(7) Cai, J.; Li, R.; Xu, X.; Zhang, L.; Lian, R.; Fang, L.; Huang, Y.; Feng, X.; Liu, X.; Li, X. CK1alpha suppresses lung tumour growth by stabilizing PTEN and inducing autophagy. *Nat. Cell Biol.* **2018**, *20* (4), 465−478.
(8) Liu, J.; Zhao, Y.; He, D.; Jones, K. M.; Tang, S.; Allison, D. B.; Zhang, Y.; Chen, J.; Zhang, Q.; Wang, X. A kinome-wide CRISPR screen identifies CK1alpha as a target to overcome enzalutamide resistance of prostate cancer. *Cell Rep. Med.* **2023**, *4* (4), 101015.
(9) Lantermann, A. B.; Chen, D.; McCutcheon, K.; Hoffman, G.; Frias, E.; Ruddy, D.; Rakiec, D.; Korn, J.; McAllister, G.; Stegmeier, F. Inhibition of Casein Kinase 1 Alpha Prevents Acquired Drug Resistance to Erlotinib in EGFR-Mutant Non-Small Cell Lung Cancer. *Cancer Res.* **2015**, *75* (22), 4937−4948.
(10) Corsello, S. M.; Zhang, H.; Rupaimoole, R.; Schulze, V. K.; Lemos, C.; Handing, K. B.; Orsi, D. L.; Shekhar, M.; Sack, U.; Christian, S.; Bone, W. Abstract 3588: Discovery of potent and selective CSNK1A1 inhibitors for solid tumor therapy. *Cancer Res.* **2022**, *82* (12_Supplement), 3588−3588.
(11) Lu, W. Targeted protein degradation bypassing cereblon and von Hippel-Lindau. *The Innovation* **2023**, *4* (3), 100422.
(12) Kronke, J.; Fink, E. C.; Hollenbach, P. W.; MacBeth, K. J.; Hurst, S. N.; Udeshi, N. D.; Chamberlain, P. P.; Mani, D. R.; Man, H. W.; Gandhi, A. K. Lenalidomide induces ubiquitination and degradation of CK1alpha in del(5q) MDS. *Nature* **2015**, *523* (7559), 183−188.
(13) Miyamoto, D. K.; Curnutt, N. M.; Park, S. M.; Stavropoulos, A.; Kharas, M. G.; Woo, C. M. Design and Development of IKZF2 and CK1alpha Dual Degraders. *J. Med. Chem.* **2023**, *66* (24), 16953−16979.
(14) Park, S.-M.; Miyamoto, D. K.; Han, G. Y. Q.; Chan, M.; Curnutt, N. M.; Tran, N. L.; Velleca, A.; Kim, J. H.; Schurer, A.; Chang, K.; Xu, W. Dual IKZF2 and CK1α degrader targets acute myeloid leukemia cells. *Cancer Cell* **2023**, *41* (4), 726−739.e11.
(15) Nishiguchi, G.; Mascibroda, L. G.; Young, S. M.; Caine, E. A.; Abdelhamed, S.; Kooijman, J. J.; Miller, D. J.; Das, S.; McGowan, K.; Mayasundari, A. Selective CK1alpha degraders exert antiproliferative activity against a broad range of human cancer cell lines. *Nat. Commun.* **2024**, *15* (1), 482.
(16) Teng, M.; Lu, W.; Donovan, K. A.; Sun, J.; Krupnick, N. M.; Nowak, R. P.; Li, Y. D.; Sperling, A. S.; Zhang, T.; Ebert, B. L. Development of PDE6D and CK1alpha Degraders through Chemical Derivatization of FPFT-2216. *J. Med. Chem.* **2022**, *65* (1), 747−756.
(17) Matyskiela, M. E.; Lu, G.; Ito, T.; Pagarigan, B.; Lu, C. C.; Miller, K.; Fang, W.; Wang, N. Y.; Nguyen, D.; Houston, J. A novel cereblon modulator recruits GSPT1 to the CRL4(CRBN) ubiquitin ligase. *Nature* **2016**, *535* (7611), 252−257.
(18) Petzold, G.; Fischer, E. S.; Thoma, N. H. Structural basis of lenalidomide-induced CK1alpha degradation by the CRL4(CRBN) ubiquitin ligase. *Nature* **2016**, *532* (7597), 127−130.
(19) (a) Rew, Y.; Sun, D. Discovery of a small molecule MDM2 inhibitor (AMG 232) for treating cancer. *J. Med. Chem.* **2014**, *57* (15), 6332−6341. (b) Foucquier, J.; Guedj, M. Analysis of drug combinations: current methodological landscape. *Pharmacol. Res. Perspect.* **2015**, *3* (3), No. e00149.

(20) Vassilev, L. T.; Vu, B. T.; Graves, B.; Carvajal, D.; Podlaski, F.; Filipovic, Z.; Kong, N.; Kammlott, U.; Lukacs, C.; Klein, C. In vivo activation of the p53 pathway by small-molecule antagonists of MDM2. *Science* **2004**, *303* (5659), 844−848.

(21) Chen, S.; Wu, J. L.; Liang, Y.; Tang, Y. G.; Song, H. X.; Wu, L. L.; Xing, Y. F.; Yan, N.; Li, Y. T.; Wang, Z. Y.; Xiao, S.-J. Arsenic Trioxide Rescues Structural p53 Mutations through a Cryptic Allosteric Site. *Cancer Cell* **2021**, *39* (2), 225−239.e8.

(22) Guiley, K. Z.; Shokat, K. M. A Small Molecule Reacts with the p53 Somatic Mutant Y220C to Rescue Wild-type Thermal Stability. *Cancer Discovery* **2023**, *13* (1), 56−69.